

Development of a NO_x emission model with seven optimized input parameters for a coal-fired boiler*

Yue-lan WANG¹, Zeng-yi MA^{†‡1}, Hai-hui YOU¹, Yi-jun TANG¹,
Yue-liang SHEN², Ming-jiang NI¹, Yong CHI¹, Jian-hua YAN¹

¹State Key Laboratory of Clean Energy Utilization, Zhejiang University, Hangzhou 310027, China

²Electric Power Research Institute of Guangdong Power Grid Corporation, Guangzhou 510080, China

[†]E-mail: mazy@zju.edu.cn

Received Dec. 21, 2016; Revision accepted June 11, 2017; Crosschecked Mar. 7, 2018

Abstract: Optimizing the operation of coal-fired power plants to reduce nitrogen oxide (NO_x) emissions requires accurate modeling of the NO_x emission process. The careful selection of input parameters not only forms the basis of accurate modeling, but can also be used to reduce the complexity of the model. The present study employs the least squares support vector machine-supervised learning method to model NO_x emissions based on historical real time data obtained from a 1000-MW once-through boiler. The initial input parameters are determined by expert knowledge and operational experience, while the final input parameters are obtained by sensitivity analysis, where the variation in model accuracy for a given set of data is analyzed as one or several input parameters are successively omitted from the calculations, while retaining all other parameters. Here, model accuracy is evaluated according to the mean relative error (MRE). This process reduces the parameters required for NO_x emission modeling from an initial number of 33 to 7, while the corresponding MRE is reduced from 3.09% to 2.23%. Moreover, a correlation of 0.9566 between predicted and measured values was obtained by applying the model with just these seven input parameters to a validation dataset. As such, the proposed method for selecting input parameters serves as a reference for related studies.

Key words: Nitrogen oxide (NO_x); Coal-fired boiler; Least squares support vector machine; Input parameters; Sensitivity analysis
<https://doi.org/10.1631/jzus.A1600787>

CLC number: TK229.6


1 Introduction

Coal-fired power plants represent a major component of electrical power generation, accounting for 41.3% of the world's electricity in 2013 (IEA, 2015). However, coal is not a clean resource, and its combustion introduces numerous undesirable air pollutants into the ambient surroundings. One of the most significant pollutants affecting the global at-

mosphere is the nitrogen oxides (NO_x), which result in damage to the environment, producing effects such as acid rain, photochemical smog, greenhouse effects, and the depletion of stratospheric ozone (Liu et al., 2011; Tang et al., 2012). These conditions not only represent severe threats to human health, but also lead to economic loss (Wei et al., 2007). Owing to the negative impact of NO_x, various technologies including selective catalytic reduction (SCR) (Wang et al., 2005; Xu et al., 2014; Xiang et al., 2015), selective non-catalytic reduction (SNCR) (Modlinski, 2015), over-fire air (Fan et al., 2010; Li et al., 2013; Kuang et al., 2014), and low-NO_x burners (Zhou et al., 2014, 2015, 2017), have been developed to control NO_x emissions. Among these technologies, the optimization of power-plant operating parameters

[‡] Corresponding author

* Project supported by the Science and Technology Plan Project of Zhejiang Province (No. 2014C33018), China

 ORCID: Zeng-yi MA, <https://orcid.org/0000-0002-4504-6198>

© Zhejiang University and Springer-Verlag GmbH Germany, part of Springer Nature 2018

offers substantial potential for reducing the NO_x emissions of coal-fired power plants based on the premise that optimized operation minimizes NO_x emissions. Moreover, optimized operation parameters are more time and cost efficient and easier to implement than other technologies (Wei et al., 2013).

The operating parameter optimization approach must first establish a model that accurately describes the relationship between NO_x emission and the operating parameters. Modeling NO_x emissions includes two main steps: the selection of the modeling approach, and the selection of the input parameters. In recent years, modeling approaches, such as principle component analysis (PCA), partial least squares (PLS), artificial neural network (ANN), support vector machine (SVM), and least squares support vector machine (LSSVM), have been intensively studied. Khajehsharifi et al. (2017) used PCA to predict the proportions of three pyrimidine bases including uracil, cytosine, and thymine when mixed together. Junhom et al. (2017) applied PLS regression combined with Fourier transform infrared (FTIR) microspectroscopy to predict the resistance to hepatocellular carcinoma. Hattori and Otsuka (2013) employed PLS regression based on the use of datasets, integrating both the near-infrared (NIR) spectra and the physical properties of granules to predict the process parameters of tablet compression, such as the displacements of upper and lower punches. PCA and PLS are used to make regression models, but they are especially suitable for linear modeling, or weak nonlinear modeling (Thissen et al., 2004; Malegori et al., 2017). The combustion process is a highly nonlinear and strong coupling process, so PCA and PLS are not suitable for modeling NO_x, whereas ANN, SVM, and LSSVM are well suited to nonlinear modeling. A back-propagation neural network (BPNN) was used to model the unburned carbon in bottom ash of a 210 MW coal-fired boiler, and a genetic algorithm (GA) was used to find the optimum operating parameters to reduce the unburned carbon in bottom ash (Ilamathi et al., 2013; Yin et al., 2017). A multilayer perceptron (MLP) was used to establish a NO_x model for a tangentially coal-fired boiler (Zhou et al., 2004). A globally enhanced general regression neural network (GE-GRNN) was developed to model multiple objectives of boilers including coal mass flow rate, NO_x, and loss on ignition (Song et al., 2017). A cas-

caded fuzzy neural network (CFNN) was employed to predict the break size of loss-of-coolant accidents (LOCAs) in nuclear power plants (Choi et al., 2017). The combination of an ANN and a particle swarm algorithm (PSO) was presented to model the dew-point pressure in retrograded condensate gas reservoirs (Ahmadi et al., 2014c). In short, the ANN has many variants and is widely used in modeling, but ANN models have difficulty obtaining a stable solution and are prone to over-fitting (Smrekar et al., 2013; Zhang and Liu, 2017). Using an SVM based on structural risk minimization, it is impossible to become trapped in local minima, and SVM has better generalization than ANN (Ahmadi et al., 2014a; Ahmadi MH et al., 2015). Zhou et al. (2012) applied SVM to model NO_x emissions from coal-fired utility boilers and compared an SVM model with BPNN and GRNN models, and the results showed that the SVM model was better. As a development of the standard SVM, LSSVM replaces the traditional quadratic programming in SVM with linear least squares criteria for the loss function. As a result, LSSVM not only inherits the advantages of SVM, including a unique solution and substantial generalization ability, but also dramatically reduces the training time, by solving a group of linear equations instead of a quadratic programming problem (Laurain et al., 2015). Owing to the advantages of LSSVM, it has been extensively applied in many fields requiring modeling, such as thermal power generation (Gu et al., 2011; Samui et al., 2015), petroleum engineering (Ahmadi and Ebadi, 2014; Ahmadi et al., 2014b, 2014d, 2015a, 2015b; Ahmadi, 2015), and chemical engineering (Ahmadi and Bahadori, 2015b; Ahmadi et al., 2015c, 2015d). Therefore, LSSVM was used in the present study.

The proper selection of input parameters can be expected to have a crucial influence on modeling results. If an inappropriate input parameter that has only a slight or even negative effect on the modeling outcome is selected, it not only increases the model's complexity, but also reduces its accuracy. Therefore, the present study focused predominantly on the selection of input parameters. The LSSVM models were trained using historical operational data obtained from a 1000-MW ultra-supercritical once-through boiler with opposed swirling burners. The initial operating parameters were selected based on expert knowledge and previous experience. However, the

final set of input parameters was determined by sensitivity analysis to provide a trade-off between the model's complexity associated with the number of input parameters and the desired accuracy of the prediction. The sensitivity analysis process reduced the parameters from an initial number of 33 to 7. The accuracy of the developed model was then verified using the remaining historical operational data. The LSSVM model based on the final seven input parameters gave sufficiently accurate predictions of NO_x emission from the modeled boiler.

In this paper, we first present a brief review of LSSVM. Then, we describe the development process for the NO_x emissions model. At last, we focus on the selection of input parameters.

2 Review of LSSVM

LSSVM was first proposed by Suykens and Vandewalle (1999) and has been described in detail elsewhere (Suykens et al., 2002). The LSSVM algorithm for nonlinear function estimation is reviewed briefly as follows.

Given a training set $\{\mathbf{x}_i, y_i\}$, $i=1, 2, \dots, N$, where $\mathbf{x}_i \in \mathbb{R}^n$ for n inputs, $y_i \in \mathbb{R}$, and N is the number of samples, the regression formula in the primal weight space is

$$\mathbf{y} = \boldsymbol{\omega}^T \boldsymbol{\varphi}(\mathbf{x}) + b, \quad (1)$$

where $\boldsymbol{\omega}$ is a weight vector, and b represents a bias term, both of which require a solution; $\boldsymbol{\varphi}(\cdot)$ maps the input parameters into a high dimensional feature space, which may even be infinite. The optimization problem for Eq. (1) when applying LSSVM can be transformed into the following form, according to the structural risk minimization:

$$\min_{\boldsymbol{\omega}, b, \mathbf{e}} J(\boldsymbol{\omega}, \mathbf{e}) = \frac{1}{2} \boldsymbol{\omega}^T \boldsymbol{\omega} + \frac{1}{2} C \sum_{i=1}^N e_i^2, \quad (2)$$

where C is a regularization parameter that seeks a trade-off between model complexity and estimation accuracy (Ahmadi and Bahadori, 2015a), and e_i is the regression error. The solution is subject to the equality constraints:

$$y_i = \boldsymbol{\omega}^T \boldsymbol{\varphi}(\mathbf{x}_i) + b + e_i, \quad i=1, 2, \dots, N. \quad (3)$$

Considering the special structure of the optimization problem, the following Lagrangian is constructed:

$$L(\boldsymbol{\omega}, b, \mathbf{e}, \boldsymbol{\alpha}) = J(\boldsymbol{\omega}, \mathbf{e}) - \sum_{i=1}^N \alpha_i \{ \boldsymbol{\omega}^T \boldsymbol{\varphi}(\mathbf{x}_i) + b + e_i - y_i \}, \quad (4)$$

where α_i is the Lagrange multiplier. Because Eq. (4) satisfies the Karush-Kuhn-Tucker conditions (Fletcher, 1987; Zhang et al., 2015), the difference equation of Eq. (4) is expressed with respect to $\boldsymbol{\omega}$, b , e_i , and α_i , respectively, and the conditions for optimality are given by

$$\begin{cases} \frac{\partial L}{\partial \boldsymbol{\omega}} = 0, \rightarrow \boldsymbol{\omega} = \sum_{i=1}^N \alpha_i y_i \boldsymbol{\varphi}(\mathbf{x}_i), \\ \frac{\partial L}{\partial b} = 0, \rightarrow \sum_{i=1}^N \alpha_i = 0, \\ \frac{\partial L}{\partial e_i} = 0, \rightarrow \alpha_i = C e_i, \quad i=1, 2, \dots, N, \\ \frac{\partial L}{\partial \alpha_i} = 0, \rightarrow \boldsymbol{\omega}^T \boldsymbol{\varphi}(\mathbf{x}_i) + b + e_i - y_i = 0, \quad i=1, 2, \dots, N. \end{cases} \quad (5)$$

After $\boldsymbol{\omega}$ and e_i are eliminated, the following solution is obtained:

$$\begin{bmatrix} 0 & \mathbf{1}_v^T \\ \mathbf{1}_v & \boldsymbol{\Omega} + \mathbf{I}/C \end{bmatrix} \begin{bmatrix} b \\ \boldsymbol{\alpha} \end{bmatrix} = \begin{bmatrix} 0 \\ \mathbf{y} \end{bmatrix}, \quad (6)$$

where $\mathbf{y}=[y_1; y_2; \dots; y_N]$, $\mathbf{1}_v=[1; 1; \dots; 1]$, $\boldsymbol{\alpha}=[\alpha_1; \alpha_2; \dots; \alpha_N]$, \mathbf{I} denotes the identity matrix, and $\boldsymbol{\Omega}$ is expressed as

$$\boldsymbol{\Omega}_{ij} = \boldsymbol{\varphi}(\mathbf{x}_i)^T \boldsymbol{\varphi}(\mathbf{x}_j) = K(\mathbf{x}_i, \mathbf{x}_j), \quad i, j=1, 2, \dots, N. \quad (7)$$

Here, $K(\mathbf{x}_i, \mathbf{x}_j)$ is the kernel function, which satisfies Mercer's conditions (Suykens et al., 2001). Therefore, the resulting LSSVM model for nonlinear function estimation becomes

$$y(x) = \sum_{i=1}^N \alpha_i K(x, x_i) + b. \quad (8)$$

3 Development of a NO_x emission model

3.1 Brief description of the boiler

The ultra-supercritical once-through boiler used in the present study has a large furnace with a cross section of 15.56 m×33.97 m and a height of 69.7 m. Fig. 1 shows a schematic of the boiler. It is equipped with six medium-speed mills, here defined as mills A, B, C, D, E, and F, where, under the rated load, five are placed into operation and one is held in reserve. Each mill is employed to supply pulverized coal to eight swirling burners in a layer. Taking the front wall as an example, three layers of swirling burners are included, which, from bottom to top, are denoted as layers A, B, and C, respectively. Two side air ports (SAPs) are fixed over the upper swirling burners, one near the left wall and the other near the right wall. Similar to the arrangement of the swirling burners, eight after air ports (AAPs) are arranged in a layer at the top. Both the SAPs and AAPs are swirling air ports. The arrangement of these nozzles in the rear wall is equivalent to that in the front wall, and the swirling burners are denoted, from bottom to top, as layers F, E, and D, respectively.

3.2 Selection of initial input parameters

The initial input parameters required for the development of a NO_x emission model using LSSVM were determined by expert knowledge and operation experience. This approach differs from the application of first principles in which the input parameters are restricted by the equations describing the mechanism, because not all possible parameters are essential. Here, NO_x emission is the only objective of the model. Because NO_x is produced mainly by the reaction of oxygen with nitrogen and its compounds, NO_x generation predominantly depends on coal and air supplies, so coal and air related parameters were selected as the initial input parameters, in addition to a minor number of other parameters. The impact of these considerations on initial parameter selection is discussed in greater detail as follows.

1. Coal. The quality and quantity of coal are the main factors affecting NO_x emission. For the quality,

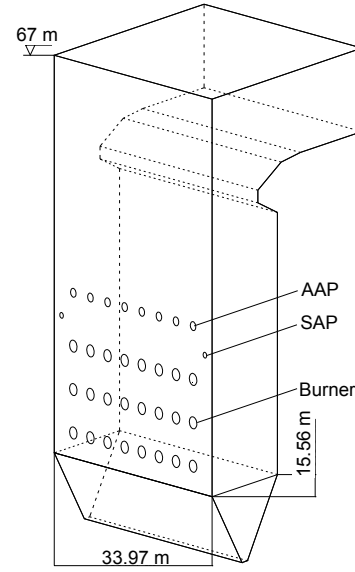


Fig. 1 Schematic of the 1000-MW ultra-supercritical once-through boiler

the carbon (C_{ad}), hydrogen (H_{ad}), oxygen (O_{ad}), nitrogen (N_{ad}), sulfur (S_{ad}), moisture content (M_t), ash (A_{ad}), volatile matter (V_{ad}) concentrations, along with the low heat value ($Q_{net,ar}$), were taken as inputs. M_t and $Q_{net,ar}$ are analyzed based on as-received basis, while the others are based on air dried basis. Similar inputs have been chosen previously (Wu et al., 2009). Note that all these values are averages because the pulverized coal provided by the mills may exhibit some variability. For the quantity, the coal feeding rates of the six mills, defined as mc_a , mc_b , mc_c , mc_d , mc_e , and mc_f , were selected as inputs (Lv et al., 2015).

2. Air. Coal-fired power plants generally employ two components of air divided according to their function, namely, primary air and secondary air. With regard to the impact of primary air on NO_x generation, the primary air flow rates of the six mills namely mp_a , mp_b , mp_c , mp_d , mp_e , and mp_f were taken as inputs. One stream, denoted as over-fire air, is separated from the secondary air for the express purpose of controlling NO_x generation. The over-fire air is employed in the SAPs and AAPs in an ultra-supercritical opposed swirling boiler. The air from the forced draught fans is distributed right and left via main air ducts to each bellow. Valves on the main air duct are responsible for adjusting the air flow by adjusting the pressure, which indicates that two valves are responsible for regulating the air flow for each bellow. Then, the air

out of the bellows passes through the swirling burners, AAPs, and SAPs, and into the furnace. Note that each AAP and SAP layer on the same side shares a bellow. Although the ports are adjustable, they are almost fixed in the operation, because frequent adjustment shortens their life. Therefore, the valve openings on the main air ducts were selected as the input parameters reflecting the impact of secondary air and over-fire air on NO_x emissions. Here, the average value of the two valve openings leading to each bellow or the air flow in each layer was regarded as a single parameter; thus, V_a , V_b , V_c , V_d , V_e , and V_f denoted valves regulating each layer of secondary air, and V_{of} and V_{or} represented valves regulating over-fire air in the front and rear walls, respectively. In addition, the total air flow rate, defined as m_{ta} , from all branches was taken as an input parameter. Valve openings for secondary air and over-fire air, and the total air flow rate, have been employed previously (Lv et al., 2013).

3. Other factors. Owing to an absence of data reflecting the temperature distribution inside a furnace, which is very difficult to measure directly, the furnace outlet temperature (T) was selected as an input parameter. In addition, because changes in the working conditions are known to result from changes in the boiler load, the boiler load (L_d) was included as an initial input parameter. Finally, the oxygen (O_2) content in the flue gas output from the furnace, which reflects the reduction or oxidation properties within the furnace, was also regarded as an input parameter. These parameters have also been applied in NO_x models elsewhere (Li et al., 2013; Lv et al., 2013).

The above analysis introduced 33 input parameters, and the initial input and output parameters for the LSSVM model are shown in Fig. 2. The final set of input parameters obtained after sensitivity analysis will be discussed in Section 4.

3.3 Data acquisition and selection

Currently, nearly all existing power plants are equipped with distributed control system (DCS). All the operational data employed in the present study, except the coal quality, were acquired from the DCS due to its numerous advantages, such as rapid collection and reduced interference with power plant operation compared to hot-state experiments. With respect to coal quality, no real-time data were obtainable owing to the unavailability of an online analyzer. However, the results of manual analysis, which could be used to perform the modeling, were recorded. Note that a time delay exists between NO_x emission and the input parameters which results mainly from the measuring device. In general, according to experience, the value of NO_x in the DCS is later by about 40–60 s than the actual value, and in the present study, the delay was taken as 50 s. Therefore, to ensure the authenticity of the model, the value of NO_x was collected 50 s after the input parameters.

At a sampling frequency of 1 min^{-1} , 21 315 operational data points were acquired over about 15 consecutive days of operation during which the boiler load varied from about 400 to 1000 MW. After the elimination of severe fluctuations in the boiler load, 1500 operational data points representative of 25 h of boiler operation were finally selected for training

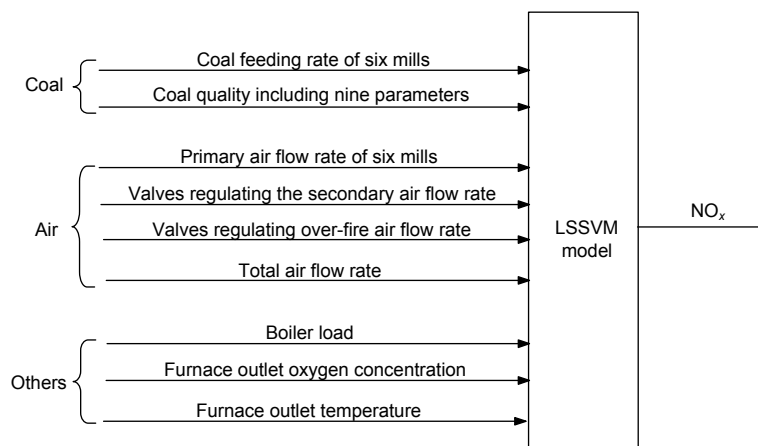


Fig. 2 Initial input and output parameters of the NO_x emission model

purposes. However, not all of the data could be used to develop a NO_x emission model, because some data are erroneous as the result of either faulty sensors or human error. These erroneous data must be identified and removed at the beginning of data selection, otherwise the prediction accuracy of the resulting model will be compromised. In addition, those data points that represent a physically improbable trend should be omitted. For example, NO_x emission will increase substantially as the oxygen content increases in the flue gas, and trends running counter to this are most likely erroneous. Data collected under unsteady conditions including boiler startup and shutdown adversely affect the LSSVM training process, and should also be omitted.

After preprocessing, 1117 operational data points were selected for model training and validation. The ranges of the input parameters are listed in Table 1. From the total, 800 rows of data were used as LSSVM training data, and the remainder for the final validation of the developed model to verify its potential usefulness in real-life applications.

3.4 Model development

The NO_x emissions model was built using the LSSVM-supervised learning method. The Gaussian radial basis function (RBF) defined in Eq. (9) was used as a kernel function in the LSSVM model. The kernel parameter σ and the regularization parameter C have a direct impact on the generalization ability and regression accuracy of the model, and both serve as kernel tuning parameters. Here, a PSO algorithm (Kennedy and Eberhart, 1995; Eberhart et al., 2001; Khajehzadeh et al., 2011; Rezaei et al., 2016) was adopted to determine the optimal combination, in which leave-one-out cross-validation was employed as the fitness function.

$$K(x, x_i) = \exp\left(-\|x - x_i\|/\sigma^2\right), \quad (9)$$

where σ is the kernel parameter and denotes the kernel width (Wang and Zhang, 2011).

4 Results and discussion

Sensitivity analysis was performed to determine the contribution made to the output by each initially selected input parameter. Input parameters with a

Table 1 Range of variation in input parameters

| Input variable | Variation range |
|---|------------------|
| Coal characteristic | |
| C _{ad} (%) (in weight) | [53.8, 57.3] |
| H _{ad} (%) (in weight) | [3.8, 4.0] |
| O _{ad} (%) (in weight) | [20.3, 26.5] |
| N _{ad} (%) (in weight) | [0.98, 1.04] |
| S _{ad} (%) (in weight) | [0.25, 0.75] |
| M _t (%) | [22.3, 25.6] |
| A _{ad} (%) | [3.4, 6.6] |
| V _{ad} (%) | [40.0, 42.5] |
| Q _{net,ar} (MJ/kg) | [19.4, 20.8] |
| Coal feeding rate (t/h) | |
| mc _a | [52.6, 80.6] |
| mc _b | [0, 79.8] |
| mc _c | [0, 78.4] |
| mc _d | [0, 79.0] |
| mc _e | [47.4, 79.8] |
| mc _f | [53.8, 57.3] |
| Primary air flow rate (t/h) | |
| mp _a | [127.8, 155.8] |
| mp _b | [10.2, 146.1] |
| mp _c | [0, 163.2] |
| mp _d | [0, 158.6] |
| mp _e | [113.6, 145.8] |
| mp _f | [113.4, 140.0] |
| Secondary air valve opening (%) | |
| V _a | [79.2, 98.6] |
| V _b | [0, 97.0] |
| V _c | [0, 95.6] |
| V _d | [78.1, 98.4] |
| V _e | [76.5, 99.2] |
| V _f | [0, 98.7] |
| Over-fire air valve opening (%) | |
| V _{of} | [0, 49.1] |
| V _{or} | [0, 48.1] |
| Other factors | |
| L _d (MW) | [397.6, 993.9] |
| m _{ta} (t/h) | [1685.1, 3306.4] |
| O ₂ content (%) (in volume) | [0.95, 4.58] |
| T (°C) | [310.2, 365.0] |
| NO _x emission (mg/m ³) | [139.2, 371.5] |

small contribution typically increase the model complexity, and can be excluded in accordance with the constraint associated with the desired model accuracy. This process was expected to significantly reduce the number of input parameters required for the LSSVM model.

The input parameters were again divided into three types: coal, air, and other factors. Here, the variation in model accuracy for a given set of data was analyzed as one or several input parameters were successively omitted from the calculations, while including all other parameters. Clearly, for accurate comparison, only the input parameters were varied, and all data associated with model training and validation had to remain unchanged for each set of input parameters. All parameters and settings employed in model training also had to remain unchanged for each set of input parameters. In addition, the outputs of all LSSVM models had to be compared according to an identical standard. Here, the mean relative error (MRE) was used to evaluate model performance, defined as

$$\text{MRE} = \frac{1}{N} \sum_{i=1}^N \left| \frac{y_i - \hat{y}_i}{y_i} \right| \times 100\%, \quad (10)$$

where y_i and \hat{y}_i are the actual measured NO_x emissions and the corresponding predicted value, respectively. In addition, each of the MRE values obtained was subjected to an averaging process involving ten repetitive computations to weaken the influence of randomness. As a result, the average value when using all initial input parameters was 3.09%, which was regarded as the base case with respect to the following analysis. Finally, in the following subsections, one or more input parameters were omitted and compared to the base case to observe the influence of individual parameters on NO_x generation. Input parameters successively omitted and defined as cases were used to prove whether coupling existed among parameters.

4.1 Effects of coal-related input parameters

Fig. 3 shows the effect of coal quality on NO_x emission. The MRE was not improved by the omission of any parameter related to coal quality. In fact, the MRE decreased with the omission of all coal quality parameters from the initial 33 input parameters (Case 1). This indicates that the coal quality has no effect on NO_x emission. Coal characteristics have a substantial impact on NO_x emission in theory. However, in practice, mixed coal is as close as possible to the designed coal quality under normal conditions,

such that the coal quality remains roughly unchanged, as shown in Table 1. This greatly limits the effect of coal quality on NO_x emission in LSSVM models.

Fig. 4 shows the effects of coal feeding rate on NO_x emission for each of the six mills. The MRE was reduced when each of these input parameters was omitted separately, and the removal of all six simultaneously reduced the MRE to 2.96%. This indicates that these six parameters had no effect on the NO_x emissions model and could be removed from the initial 33 input parameters. The generation of NO_x is a very complex nonlinear coupling process, and the feeding rate has little effect on NO_x production if the combustion is good, i.e. if it has a proper ratio of secondary air, a good furnace outlet oxygen concentration, and a suitable furnace temperature. For example, NO_x emission was equivalently 200 mg/m^3 under both 953-MW and 654-MW loads, although the

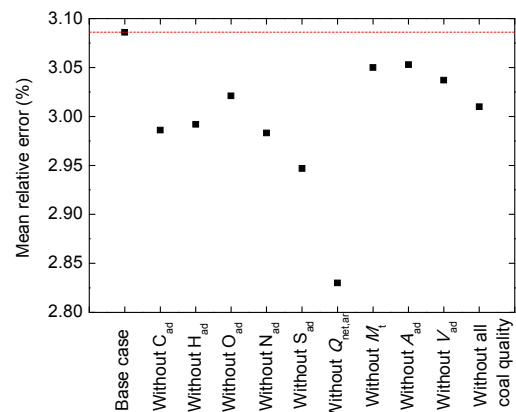


Fig. 3 Effects of coal quality on MRE for model predictions of NO_x emission

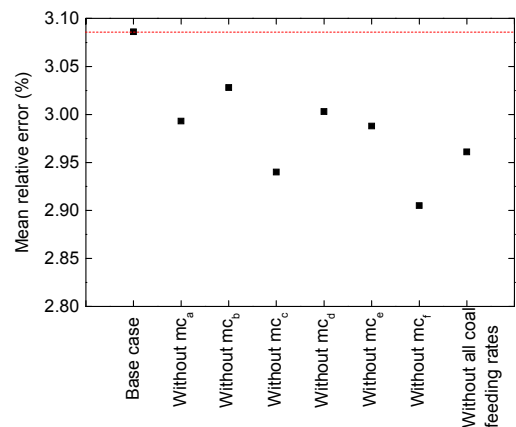


Fig. 4 Effects of coal feeding rates on MRE for model predictions of NO_x emission

coal feeding rates were different. The 953-MW load involved a feeding rate of about 61 t/h for each of the six mills, while in the case of the 654-MW load the upper mill in the rear wall was out of service, the feeding rate of the upper mill in the front wall was 46 t/h, and those of the lower and medium mills in the front and rear walls were each about 61 t/h. In addition, in Case 2, in which the coal feeding rates of all six mills from Case 1 were removed, the MRE was reduced further to 2.92%.

According to the results, all of the coal-related parameters could be removed from input parameters.

4.2 Effects of air related input parameters

Fig. 5 presents the MRE variation with the primary air flow omitted. Comparison with Fig. 4 indicates that the impact of the primary air flow of each mill was mostly consistent with that of the coal feeding rate. The MRE became smaller compared to the base case when the primary air flows of the six mills were removed from the initial 33 input parameters. This is because the primary air flow was calculated according to an appropriate coal to air ratio based on a given coal feeding rate. Moreover, on the basis of Case 2, the MRE decreased from 2.92% to 2.35% with the removal of the primary air flows of all mills (Case 3). This not only reduces the MRE by as much as 0.57 percentage points, but also reduces the input parameters by six, which substantiates the effectiveness of the sensitivity analysis.

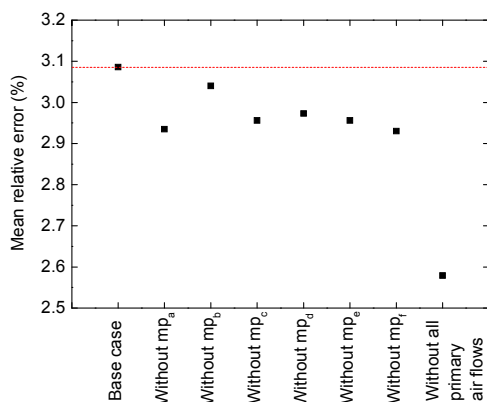


Fig. 5 Effects of the primary air flows on MRE for model predictions of NO_x emission

When the valve regulating each secondary air layer was omitted from the input parameters, the

resulting MRE values were shown in Fig. 6a. All MREs in the six cases were smaller than that of the base case, indicating that any individual level of secondary air omitted had no effect on NO_x generation. Then, the influences of any two, three, and up to six valve parameters on NO_x generation were evaluated to obtain the appropriate number. The resulting MRE values are given in Figs. 6b, 6c, and 6d, respectively, for the cases where two, three, and four valves of the six secondary air layers were omitted. Compared to the base case, the MRE was reduced under some conditions in Figs. 6b and 6c, while in Fig. 6d, all of the MREs are greater. This indicates that half of the valve parameters should be retained, including the combinations $V_f, V_a,$ and V_b ; $V_f, V_a,$ and V_c ; $V_f, V_a,$ and V_d ; $V_f, V_b,$ and V_c ; $V_f, V_b,$ and V_d ; $V_f, V_b,$ and V_e ; $V_f, V_c,$ and V_d ; $V_f, V_c,$ and V_e . To determine which three valve parameters should be retained, on the basis of Case 3, each of these eight combinations was omitted individually. The results (Fig. 7) show that the MRE of only one combination, $V_f, V_b,$ and V_c , was much lower than that of Case 3. Therefore, the three parameters $V_f, V_b,$ and V_c were retained. Case 4 was defined based on the omission of $V_e, V_a,$ and V_d from Case 3. The MRE was 2.24% (Fig. 7).

Fig. 8 presents the effect of over-fire air on NO_x emission. Relative to the base case, the MRE increased without the valve regulating over-fire air in the rear wall, and decreased without it in the front wall. Therefore, in Case 5, which removes the valve regulating over-fire air in the front wall and retains the valve in the rear wall on the basis of Case 4, the MRE decreased to 2.2%, indicating the over-fire air in the rear wall had a significant impact on NO_x emission. In operation, valve regulation of the over-fire air flow in the front and rear walls was nearly equivalent over time. However, a furnace arch was located over the AAP in the rear wall (Fig. 1). This furnace arch increased the residence time of the pulverized coal in the furnace, thereby strengthening the mixing of the flue gas. This increased the role of over-fire air in the rear wall in NO_x generation, particularly for a boiler employing swirling flame burners. In contrast, because the flue gas directly entered the horizontal flue gas duct after passing through the over-fire air zone in the front wall, the furnace arch had almost no effect on the flue gas from the front wall. This contributed to its reduced role in NO_x generation.

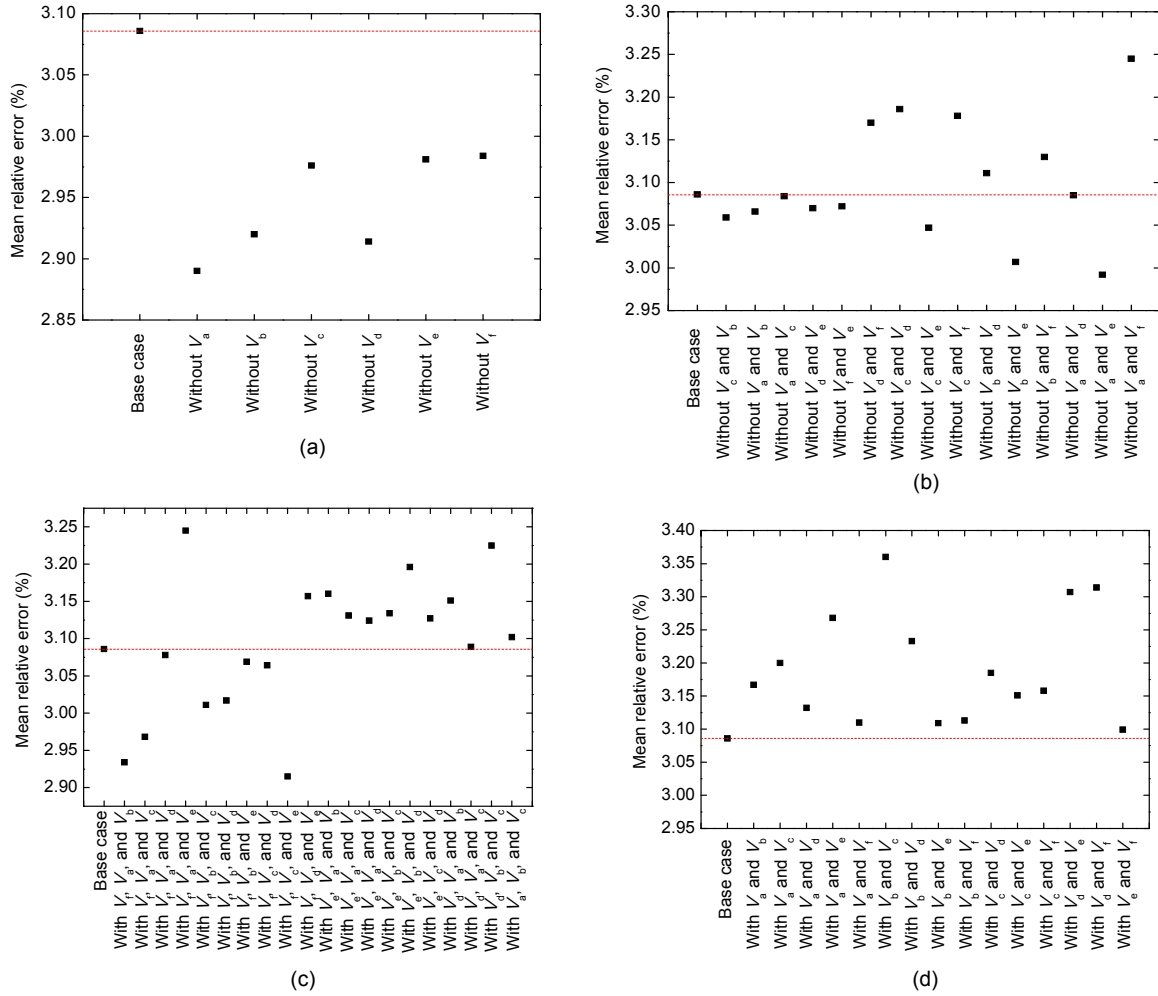


Fig. 6 Effects of only the valves regulating secondary air layers on MRE for model predictions of NO_x emission (a) One valve parameter omitted; (b) Two valve parameters omitted; (c) Three valve parameters omitted; (d) Four valve parameters omitted

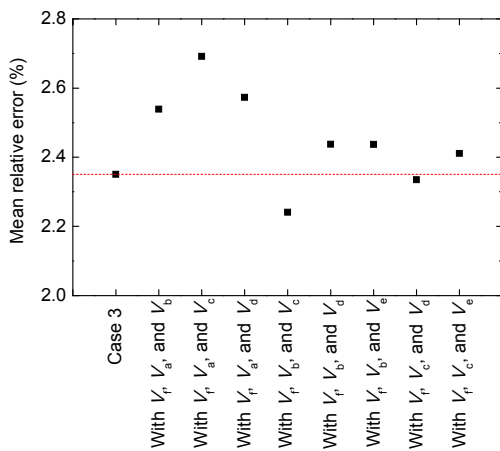


Fig. 7 MRE variation with omission of three specified valves regulating secondary air layers for model predictions of NO_x emission on the basis of Case 3

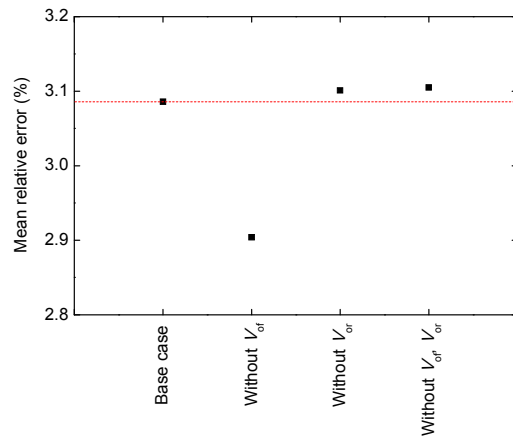


Fig. 8 Effects of the over-fire air flow on MRE for model predictions of NO_x emission

Finally, when the total air flow was omitted, based on the base case, the MRE decreased to 2.94%, while based on Case 5 (herein denoted as Case 6) the MRE increased slightly from 2.20% for Case 5 to 2.23%. This means that the total air flow was coupled with other parameters. However, since the increase was very slight, it indicated that the effect of the total air flow on NO_x emission was negligible. Therefore, the total air flow could be removed from the initial input parameters.

In this subsection, regarding the air-related input parameters, four valve parameters were retained, three of which regulate the secondary air, and one of which regulates the over-fire air in the rear wall.

4.3 Effects of other input parameters

Fig. 9 shows the variation in MRE in the absence of each of the input parameters reflecting boiler load, furnace outlet oxygen concentration, and furnace outlet temperature. The furnace outlet oxygen concentration had the greatest impact on the NO_x emission model among all other parameters considered. With the omission of furnace outlet oxygen concentration, the MRE increased 17.6% relative to that with all parameters included. The fact that nearly all types of NO_x , including fuel NO_x , thermal NO_x , and prompt NO_x , are produced by the oxidation of nitrogen or nitrogen compounds indicates the importance of oxygen. A reduced furnace outlet oxygen concentration means that less oxygen is available for the oxidation of nitrogen, reduction of NO_x is enhanced in the fuel-rich zone, and thus NO_x formation is reduced (Hill and Smoot, 2000). In addition, of all the parameters considered, other than the furnace outlet oxygen concentration, the furnace outlet temperature had the greatest impact on NO_x emission. NO_x production is highly influenced by temperature, particularly thermal NO_x . Thermal NO_x makes the largest contribution to NO_x emission after fuel NO_x , accounting for 15%–25% of the total, and its formation rate increases exponentially with increasing furnace temperature (Choi and Kim, 2009). For a furnace temperature in excess of 1500 °C, the rate of thermal NO_x formation increases by a factor of 6–7 for a temperature increase of 100 °C (Cen et al., 2003). Therefore, both the furnace outlet oxygen concentration and temperature must be retained as inputs to the model.

Finally, when only the boiler load was omitted from the input parameters, the MRE decreased. However, if it is omitted on the basis of Case 5, denoted as Case 7, the MRE increased from 2.2% to 2.58%, as seen in Fig. 10, where the MRE values of all cases including the base case through Case 7 are compared. This indicates that the boiler load was coupled with some omitted parameters. To determine the parameters related to the boiler load, the parameters omitted in Cases 1 to 6 were separately omitted together with the boiler load. We found that, except for the primary air flow, all the parameters were related to the boiler load, particularly the secondary air. Therefore, the correlated influence requires retaining the boiler load, along with the furnace outlet oxygen concentration and furnace outlet temperature.

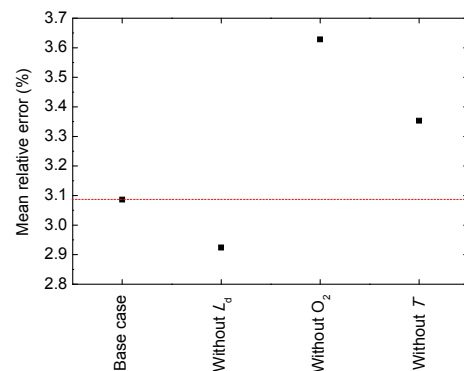


Fig. 9 Effects of boiler load, furnace outlet oxygen concentration, and furnace outlet temperature on MRE for model predictions of NO_x emission

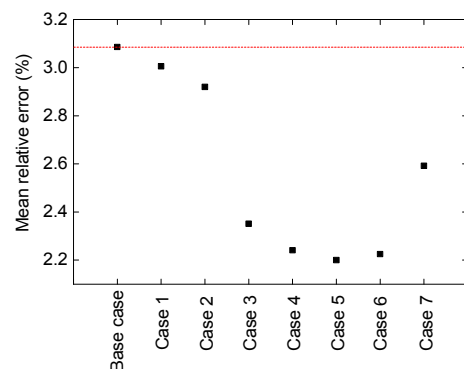


Fig. 10 MRE values of all cases from the base case to Case 7

4.4 Final input parameters of LSSVM model

According to the analysis presented in Sections 4.1–4.3, the number of the final input parameters was

reduced to seven (Fig. 11), including the valves regulating the F, B, and C layers of secondary air, the valve regulating the over-fire air flow in the rear wall, the boiler load, the furnace outlet oxygen concentration, and the furnace outlet temperature. The NO_x emission model developed with the seven input parameters was applied to the 317 rows of validation data. The prediction results are shown in Fig. 12. The MRE was 2.23% and the correlation between the predicted and measured values was 0.9566. Compared to other NO_x emission models developed using LSSVM with variable numbers of the input parameters listed in Table 2, higher accuracy was achieved, and fewer input parameters were employed.

5 Conclusions

Recently, the optimization of operating parameters has been extensively studied with the aim of reducing the NO_x emissions of coal-fired power plants. However, this approach cannot be applied in the absence of an accurate NO_x emission model to establish the relationship between input parameters and the output objective. As such, accurate selection of significant input parameters is the crucial component of any NO_x emission model. In this paper, the LSSVM-supervised learning method was used to build a NO_x emission model based on data obtained from a 1000-MW ultra-supercritical once-through boiler with swirling burners. The initial 33 input parameters were selected according to expert knowledge and operation experience. Sensitivity analysis, which seeks a trade-off between the accuracy and the complexity of a model, was employed to determine the most significant input parameters affecting NO_x emission, and the final seven input parameters were obtained: the boiler load, the furnace outlet oxygen concentration, the furnace outlet temperature, the valves regulating the upper and middle secondary air layers in the front wall and the lower secondary air layer in the rear wall, and the valve regulating the over-fire air flow in the rear wall. The MRE of the NO_x emission model developed with these seven input parameters decreased to 2.23% from the value of 3.09% obtained with all 33 input parameters. In addition, when modeling the NO_x emission using the

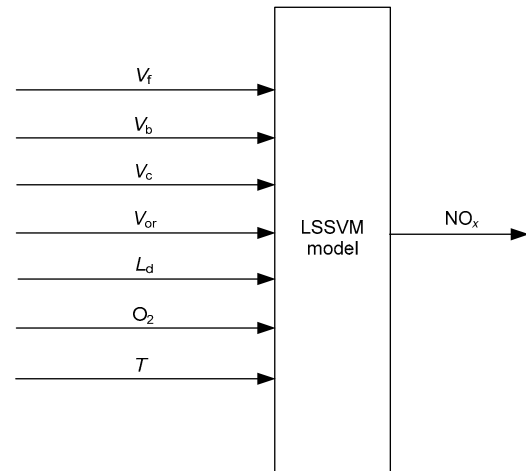


Fig. 11 Final input and output parameters for the NO_x emission model

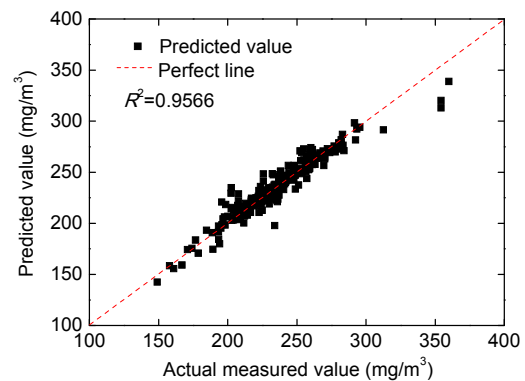


Fig. 12 Comparison between actual measured and predicted NO_x emission values for the validation dataset

Table 2 Comparison between the current study and several previous studies

| Study | Number of input parameters | MRE (%) |
|--------------------|----------------------------|---------|
| Lv et al., 2013 | 27 | 7.5 |
| Lv et al., 2015 | 19 | 9.02 |
| Ahmed et al., 2015 | 43 | 5.88 |
| Current study | 7 | 2.23 |

final seven input parameters, a correlation of 0.9566 was obtained between the model predictions and the measured values in the validation dataset. Therefore, the proposed approach for selecting significant input parameters provides a useful reference for the future modeling of other optimized systems in addition to coal-fired power plants.

References

- Ahmadi MA, 2015. Connectionist approach estimates gas–oil relative permeability in petroleum reservoirs: application to reservoir simulation. *Fuel*, 140:429-439. <https://doi.org/10.1016/j.fuel.2014.09.058>
- Ahmadi MA, Ebadi M, 2014. Evolving smart approach for determination dew point pressure through condensate gas reservoirs. *Fuel*, 117:1074-1084. <https://doi.org/10.1016/j.fuel.2013.10.010>
- Ahmadi MA, Bahadori A, 2015a. A LSSVM approach for determining well placement and conning phenomena in horizontal wells. *Fuel*, 153:276-283. <https://doi.org/10.1016/j.fuel.2015.02.094>
- Ahmadi MA, Bahadori A, 2015b. Prediction performance of natural gas dehydration units for water removal efficiency using a least square support vector machine. *International Journal of Ambient Energy*, 37(5):486-494. <https://doi.org/10.1080/01430750.2015.1004105>
- Ahmadi MA, Ebadi M, Hosseini SY, 2014a. Prediction breakthrough time of water coning in the fractured reservoirs by implementing low parameter support vector machine approach. *Fuel*, 117:579-589. <https://doi.org/10.1016/j.fuel.2013.09.071>
- Ahmadi MA, Ebadi M, Marghmaleki PS, et al., 2014b. Evolving predictive model to determine condensate-to-gas ratio in retrograded condensate gas reservoirs. *Fuel*, 124:241-257. <https://doi.org/10.1016/j.fuel.2014.01.073>
- Ahmadi MA, Ebadi M, Yazdanpanah A, 2014c. Robust intelligent tool for estimation dew point pressure in retrograded condensate gas reservoirs: application of particle swarm optimization. *Journal of Petroleum Science and Engineering*, 123:7-19. <https://doi.org/10.1016/j.petrol.2014.05.023>
- Ahmadi MA, Masoumi M, Askarinezhad R, 2014d. Evolving connectionist model to monitor the efficiency of an in situ combustion process: application to heavy oil recovery. *Energy Technology*, 2(9-10):811-818. <https://doi.org/10.1002/ente.201402043>
- Ahmadi MA, Zahedzadeh M, Shadizadeh SR, et al., 2015a. Connectionist model for predicting minimum gas miscibility pressure: application to gas injection process. *Fuel*, 148:202-211. <https://doi.org/10.1016/j.fuel.2015.01.044>
- Ahmadi MA, Masoumi M, Askarinezhad R, 2015b. Evolving smart model to predict the combustion front velocity for in situ combustion. *Energy Technology*, 3(2):128-135. <https://doi.org/10.1002/ente.201402104>
- Ahmadi MA, Hasanvand MZ, Bahadori A, 2015c. A least-squares support vector machine approach to predict temperature drop accompanying a given pressure drop for the natural gas production and processing systems. *International Journal of Ambient Energy*, 38(2):122-129. <https://doi.org/10.1080/01430750.2015.1055515>
- Ahmadi MA, Lee M, Bahadori M, 2015d. Prediction of a solid desiccant dehydrator performance using least squares support vector machines algorithm. *Journal of the Taiwan Institute of Chemical Engineers*, 50:115-122. <https://doi.org/10.1016/j.jtice.2014.12.004>
- Ahmadi MH, Ahmadi MA, Sadatsakkak SA, et al., 2015. Connectionist intelligent model estimates output power and torque of stirling engine. *Renewable and Sustainable Energy Reviews*, 50:871-883. <https://doi.org/10.1016/j.rser.2015.04.185>
- Ahmed F, Cho HJ, Kim JK, et al., 2015. A real-time model based on least squares support vector machines and output bias update for the prediction of NO_x emission from coal-fired power plant. *Korean Journal of Chemical Engineering*, 32(6):1029-1036. <https://doi.org/10.1007/s11814-014-0301-2>
- Cen KF, Yao Q, Luo ZY, et al., 2003. *Advanced Combustion*. Zhejiang University Press, Hangzhou, China (in Chinese).
- Choi CR, Kim CN, 2009. Numerical investigation on the flow, combustion and NO_x emission characteristics in a 500 MW_e tangentially fired pulverized-coal boiler. *Fuel*, 88(9):1720-1731. <https://doi.org/10.1016/j.fuel.2009.04.001>
- Choi GP, Yoo KHY, Back JH, et al., 2017. Estimation of LOCA break size using cascaded fuzzy neural networks. *Nuclear Engineering and Technology*, 49(3):495-503. <https://doi.org/10.1016/j.net.2016.11.001>
- Eberhart RC, Shi Y, Kennedy J, 2001. *Swarm Intelligence*. Morgan Kaufmann, San Francisco, USA.
- Fan WD, Lin ZC, Li YY, et al., 2010. Experimental flow field characteristics of OFA for large-angle counter flow of fuel-rich jet combustion technology. *Applied Energy*, 87(8):2737-2745. <https://doi.org/10.1016/j.apenergy.2010.02.012>
- Fletcher R, 1987. *Practical Methods of Optimization*. John Wiley & Son, Chichester and New York.
- Gu YP, Zhao WJ, Wu ZS, 2011. Online adaptive least squares support vector machine and its application in utility boiler combustion optimization systems. *Journal of Process Control*, 21(7):1040-1048. <https://doi.org/10.1016/j.jprocont.2011.06.001>
- Hattori Y, Otsuka M, 2013. Modeling of feed-forward control using the partial least squares regression method in the tablet compression process. *International Journal of Pharmaceutics*, 524(1-2):407-413. <https://doi.org/10.1016/j.ijpharm.2017.04.004>
- Hill SC, Smoot LD, 2000. Modeling of nitrogen oxides formation and destruction in combustion systems. *Progress in Energy and Combustion Science*, 26(4-6):417-458. [https://doi.org/10.1016/S0360-1285\(00\)00011-3](https://doi.org/10.1016/S0360-1285(00)00011-3)
- IEA (International Energy Agency), 2015. *Key World Energy Statistic*. IEA.
- Ilamathi P, Selladurai V, Balamurugan K, 2013. Modeling and optimization of unburned carbon in coal-fired boiler using artificial neural network and genetic algorithm. *Journal of Energy Resources Technology*, 135(3):032201. <https://doi.org/10.1115/1.4023328>
- Junhom C, Weerapreeyakul N, Tanthanuch W, et al., 2017.

- Partial least squares regression and Fourier transform infrared (FTIR) microspectroscopy for prediction of resistance in hepatocellular carcinoma HepG2 cells. *Experimental Cell Research*, 351(1):82-90.
<https://doi.org/10.1016/j.yexcr.2016.12.027>
- Kennedy J, Eberhart R, 1995. Particle swarm optimization. Proceedings of ICNN'95—International Conference on Neural Networks, p.1942-1948.
<https://doi.org/10.1109/ICNN.1995.488968>
- Khajehsharifi H, Eskandari Z, Sareban N, 2017. Using partial least squares and principal component regression in simultaneous spectrophotometric analysis of pyrimidine bases. *Arabian Journal of Chemistry*, 10(S1):S141-S147.
<https://doi.org/10.1016/j.arabjc.2012.07.015>
- Khajehzadeh M, Taha MR, El-shafie A, et al., 2011. Modified particle swarm optimization for optimum design of spread footing and retaining wall. *Journal of Zhejiang University-SCIENCE A (Applied Physics & Engineering)*, 12(6):415-427.
<https://doi.org/10.1631/jzus.A1000252>
- Kuang M, Li ZQ, Wang ZH, et al., 2014. Combustion and NO_x emission characteristics with respect to staged-air damper opening in a 600 MW_e down-fired pulverized coal furnace under deep-air-staging conditions. *Environmental Science & Technology*, 48(1):837-844.
<https://doi.org/10.1021/es403165f>
- Laurain V, Tóth R, Piga D, et al., 2015. An instrumental least squares support vector machine for nonlinear system identification. *Automatica*, 54:340-347.
<https://doi.org/10.1016/j.automatica.2015.02.017>
- Li ZQ, Liu ZC, Chen ZC, et al., 2013. Effect of angle of arch-supplied overfire air on flow, combustion characteristics and NO_x emissions of a down-fired utility boiler. *Energy*, 59:377-386.
<https://doi.org/10.1016/j.energy.2013.06.020>
- Liu FD, He H, Zhang CB, et al., 2011. Mechanism of the selective catalytic reduction of NO_x with NH₃ over environmental-friendly iron titanate catalyst. *Catalysis Today*, 175(1):18-25.
<https://doi.org/10.1016/j.cattod.2011.02.049>
- Lv Y, Liu JZ, Yang TT, et al., 2013. A novel least squares support vector machine ensemble model for NO_x emission prediction of a coal-fired boiler. *Energy*, 55:319-329.
<https://doi.org/10.1016/j.energy.2013.02.062>
- Lv Y, Yang TT, Liu JZ, 2015. An adaptive least squares support vector machine model with a novel update for NO_x emission prediction. *Chemometrics and Intelligent Laboratory Systems*, 145:103-113.
<https://doi.org/10.1016/j.chemolab.2015.04.006>
- Malegori C, Malegori EJN, de Freitas ST, et al., 2017. Comparing the analytical performances of micro-NIR and FT-NIR spectrometers in the evaluation of acerola fruit quality, using PLS and SVM regression algorithms. *Talanta*, 165:112-116.
<https://doi.org/10.1016/j.talanta.2016.12.035>
- Modlinski N, 2015. Numerical simulation of SNCR (selective non-catalytic reduction) process in coal fired grate boiler. *Energy*, 92:67-76.
<https://doi.org/10.1016/j.energy.2015.03.124>
- Rezaei H, Nazir R, Momeni E, 2016. Bearing capacity of thin-walled shallow foundations: an experimental and artificial intelligence-based study. *Journal of Zhejiang University-SCIENCE A (Applied Physics & Engineering)*, 17(4):273-285.
<https://doi.org/10.1631/jzus.A1500033>
- Samui P, Kim D, Aiyer BG, 2015. Pullout capacity of small ground anchor: a least square support vector machine approach. *Journal of Zhejiang University-SCIENCE A (Applied Physics & Engineering)*, 16(4):295-301.
<https://doi.org/10.1631/jzus.A1200260>
- Smrekar J, Potočnik P, Senegačnik A, 2013. Multi-step-ahead prediction of NO_x emissions for a coal-based boiler. *Applied Energy*, 106:89-99.
<https://doi.org/10.1016/j.apenergy.2012.10.056>
- Song JG, Romero CE, Yao Z, et al., 2017. A globally enhanced general regression neural network for on-line multiple emissions prediction of utility boiler. *Knowledge-Based Systems*, 118:4-14.
<https://doi.org/10.1016/j.knosys.2016.11.003>
- Suykens JAK, Vandewalle J, 1999. Least squares support vector machine classifiers. *Neural Processing Letters*, 9(3):293-300.
<https://doi.org/10.1023/A:1018628609742>
- Suykens JAK, Vandewalle J, de Moor B, 2001. Optimal control by least squares support vector machine. *Neural Networks*, 14(1):23-25.
[https://doi.org/10.1016/S0893-6080\(00\)00077-0](https://doi.org/10.1016/S0893-6080(00)00077-0)
- Suykens JAK, Gestel TV, Brabanter JD, et al., 2002. Least squares support vector machines. *Euphytica*, 2(2):1599-1604.
- Tang Y, Ma X, Lai Z, et al., 2012. NO_x and SO₂ emissions from municipal solid waste (MSW) combustion in CO₂/O₂ atmosphere. *Energy*, 40(1):300-306.
<https://doi.org/10.1016/j.energy.2012.01.070>
- Thissen U, Pepers M, Üstün B, et al., 2004. Comparing support vector machines to PLS for spectral regression applications. *Chemometrics and Intelligent Laboratory Systems*, 73(2):169-179.
<https://doi.org/10.1016/j.chemolab.2004.01.002>
- Wang QC, Zhang JZ, 2011. Wiener model identification and nonlinear model predictive control of a pH neutralization process based on Laguerre filters and least squares support vector machines. *Journal of Zhejiang University-SCIENCE C (Computers & Electronics)*, 12(1):25-35.
<https://doi.org/10.1631/jzus.C0910779>
- Wang ZH, Zhou JH, Zhang YW, et al., 2005. Experiment and mechanism investigation on advanced reburning for NO_x reduction: influence of CO and temperature. *Journal of Zhejiang University-SCIENCE*, 6B(3):187-194.
<https://doi.org/10.1631/jzus.2005.B0187>
- Wei ZB, Li XL, Xu LJ, et al., 2013. Comparative study of computational intelligence approaches for NO_x reduction

- of coal-fired boiler. *Energy*, 55:683-692.
<https://doi.org/10.1016/j.energy.2013.04.007>
- Wei ZS, Du ZY, Lin ZH, et al., 2007. Removal of NO_x by microwave reactor with ammonium bicarbonate and Ga-A zeolites at low temperature. *Energy*, 32(8):1455-1459.
<https://doi.org/10.1016/j.energy.2006.11.007>
- Wu F, Zhou H, Ren T, et al., 2009. Combining support vector regression and cellular genetic algorithm for multi-objective optimization of coal-fired utility boilers. *Fuel*, 88(10):1864-1870.
<https://doi.org/10.1016/j.fuel.2009.04.023>
- Xiang J, Wang PY, Su S, et al., 2015. Control of NO and Hg⁰ emissions by SCR catalysts from coal-fired boiler. *Fuel Processing Technology*, 135:168-173.
<https://doi.org/10.1016/j.fuproc.2014.12.044>
- Xu YY, Zhang Y, Liu FN, et al., 2014. CFD analysis on the catalyst layer breakage failure of an SCR-DeNO_x system for a 350 MW coal-fired power plant. *Computers & Chemical Engineering*, 69:119-127.
<https://doi.org/10.1016/j.compchemeng.2014.07.012>
- Yin F, Luo ZH, Li Y, et al., 2017. Coal type identification based on the emission spectra of a furnace flame. *Journal of Zhejiang University-SCIENCE A (Applied Physics & Engineering)*, 18(2):113-123.
<https://doi.org/10.1631/jzus.A1500306>
- Zhang JH, Liu Y, 2017. Application of complete ensemble intrinsic time-scale decomposition and least-square SVM optimized using hybrid DE and PSO to fault diagnosis of diesel engines. *Journal of Zhejiang University-SCIENCE B (Biomedicine & Biotechnology)*, 18(3):272-286.
<https://doi.org/10.1631/jzus.B1600315>
- Zhang Y, Li H, Wang ZH, et al., 2015. A preliminary study on time series forecast of fair-weather atmospheric electric field with WT-LSSVM method. *Journal of Electrostatics*, 75:85-89.
<https://doi.org/10.1016/j.elstat.2015.03.005>
- Zhou H, Cen KF, Fan JR, 2004. Modeling and optimization of the NO_x emission characteristics of a tangentially fired boiler with artificial neural networks. *Energy*, 29(1):167-183.
<https://doi.org/10.1016/j.energy.2003.08.004>
- Zhou H, Zhao JP, Zheng LG, et al., 2012. Modeling NO_x emissions from coal-fired utility boilers using support vector regression with ant colony optimization. *Engineering Applications of Artificial Intelligence*, 25(1):147-158.
<https://doi.org/10.1016/j.engappai.2011.08.005>
- Zhou H, Yang Y, Dong K, et al., 2014. Influence of the gas particle flow characteristics of a low-NO_x swirl burner on the formation of high temperature corrosion. *Fuel*, 134:595-602.
<https://doi.org/10.1016/j.fuel.2014.06.027>
- Zhou H, Yang Y, Wang YY, 2015. Numerical investigation of gas-particle flow in the primary air pipe of low NO_x swirl burner—the DEM-CFD method. *Particuology*, 19:133-140.
<https://doi.org/10.1016/j.partic.2014.04.017>
- Zhou H, Li Y, Tang Q, et al., 2017. Combining flame monitoring techniques and support vector machine for the online identification of coal blends. *Journal of Zhejiang University-SCIENCE A (Applied Physics & Engineering)*, 18(9):677-689.
<https://doi.org/10.1631/jzus.A1600454>

中文概要

题目: 基于七个运行参数建立煤粉锅炉 NO_x 排放模型

目的: 采用最小二乘支持向量机建立煤粉锅炉 NO_x 排放模型, 即建立输入参数与 NO_x 之间的关系。合理选择输入参数不仅会降低模型的复杂度, 而且会提高模型的精度。为此, 本文探讨各输入参数对模型的影响, 并最终保留合适数量的输入参数建立 NO_x 排放模型。

创新点: 1. 采用最小二乘支持向量机建立 NO_x 排放模型;
 2. 通过敏感性分析确定模型的最终输入参数。

方法: 1. 根据专家知识及运行经验确定 NO_x 排放模型的初始输入参数 (图 2); 2. 根据锅炉的运行历史数据, 采用最小二乘支持向量机建立 NO_x 排放模型;
 3. 采用敏感性分析方法确定 NO_x 排放模型的最终输入参数 (图 11), 并用其进行建模以验证模型的有效性。

结论: 1. 采用最小二乘支持向量机建立的 1000 MW 超超临界前后墙对冲锅炉 NO_x 排放模型, 可靠性和精度较高; 2. 经过敏感性分析, NO_x 排放模型的输入参数由初始的 33 个降为 7 个, 模型的复杂度降低且精度提高。

关键词: 氮氧化物; 煤粉锅炉; 最小二乘支持向量机; 输入参数; 敏感性分析